ISBN: 978-3-95450-231-8 ISSN: 2673-5490 doi: 10.18429/JACoW-IPAC2023-WEODC2

NOVEL IRON LAMINATION FOR FAST KICKER MAGNETS WITH HIGH FLUX DENSITY

K. Fukami†,[1], S. Takano[1], T. Taniuchi, T. Watanabe[1], H. Yamaguchi, JASRI, Sayo, 679-5198, Japan
T. Inagaki, H. Tanaka, RIKEN SPring-8 Center, Sayo, Hyogo 679-5148, Japan
T. Iwashita, N. Nishimori, QST, Sendai, Miyagi 980-8579, Japan
H. Nakanishi, Y. Takemura, SPring-8 Service Co., Ltd., Tatsuno, Hyogo 679-5165, Japan
[1]also at RIKEN SPring-8 Center, Sayo, Hyogo 679-5148, Japan

Abstract

Novel iron lamination with additional interlaminar insulation has been developed for magnet cores of fast kicker magnets in particle accelerators. By eliminating accidental interlaminar shorts, the eddy current induced between core laminas was minimized and the pulse profile of the excited magnetic field has been significantly improved up to a few MHz range. The magnet core is formed by alternately stacking thin steel and insulation sheets to avoid electrical contact between the steel sheets on the edge. A pair of test magnets with the new iron lamination was assembled to evaluate magnet performances focusing on applications to matched kickers in the accelerators. The magnetic field pulse profiles of the two magnets have proved to match with discrepancies of less than ±0.1 % over the entire pulse duration, which is significantly better than those with conventional iron lamination. The developed fast kicker magnets are promising for the beam injection kickers in the next-generation light sources and future colliders, where suppression of the transient stored-beam oscillation during beam injection is crucial.

INTRODUCTION

In particle accelerators, fast pulsed magnets are widely used as kickers and septa that deflect the particle beam in ejection, switching the beam delivery route, and injection. To suppress the eddy current in the core of the fast pulsed magnets, a laminated steel sheet core [1-3] or a ferrite core [4-7] is generally used. One of the advantages of the laminated steel sheet core is its larger saturation flux density than the ferrite. For example, the saturation flux density of the non-oriented silicon steel sheet, Nikkindenji Kogyo Co., Ltd., ST series, is as high as 1.6 T [8] while that of the Mn–Zn-based ferrite, TDK Ltd., PC47, is 0.6 T [9]. The high saturation flux density in the laminated steel sheet core is suitable to high field compact magnets that are extensively demanded by next-generation light sources as well as future high-energy colliders.

Some applications of the fast kicker magnets in the accelerators require matched amplitude, timing, and time profile of the magnetic field among two or more kicker magnets. In synchrotron radiation sources, the top-up operation provides the constant photon beam to beamline users [10-12]. In order for the photon users to continuously detect the light without a break during the injection timing to fully exploit the delivered photons, the stored beam has to be stable even during the beam injection. In the case of a conventional off-axis beam injection, a horizontal orbit bump is generated using pulsed kicker magnets. Matched kicker magnets are necessary to minimize the transient horizontal oscillation of the stored beam at beam injection. Although factors such as the uneven metallic coating on the inner surface of the ceramic chambers at the pulsed magnets and the leakage field from the septa can affect the amplitude of the horizontal oscillation, the matched pulsed field waveform between the kickers is essential.

In this study, we propose a novel iron lamination scheme with additional interlaminar insulation for the magnet core of fast pulsed magnets. A laminated steel sheet core is formed by alternately stacking thin steel and insulation sheets. We fabricated two test kicker magnets with the new iron lamination. The frequency dependence of the inductance of the magnets was measured up to the order of MHz, and subsequently, the difference between the two magnets was thoroughly analyzed. We also investigated the mismatch in the magnetic field waveform between the two magnets.

MAGNET DESIGN

The primary parameters are listed in Table 1. The test magnets are C-shaped magnets with a gap of 22 mm [13]. The silicon steel sheet thickness of 0.1 mm (Nikkindenji Kogyo Co., Ltd., ST-100) was selected as a core material because the thinner the silicon steel sheet laminated, the less the eddy current induced in the core. In the conventional method, a magnetic core is formed simply by stacking cut steel sheets. Although the surface of the silicon steel sheet is coated with an insulator layer of a few microns typically, the insulating layer can unintentionally peel off from the edge during the cutting process to fit the core cross-section shape. Furthermore, some burrs can occur around the edge. As a result, unexpected electrical contact between the steel sheets can occur on the edges, leading to unspecified eddy current in the core at the magnet excitations.

To avoid electrical contacts on the edge of the cut steel sheets, we decided to insert a thin insulating sheet of polyimide between each piece of the steel sheet. Inspection of the edges of the cut steel sheets revealed that the maximum burr size was 0.002 mm. We need a larger thickness for the polyimide sheet than the maximum burr size. On the other hand, the thicker the insulating sheet inserted, the higher the reduction in the core packing factor. Therefore, the thickness of 0.025 mm was selected as the optimal solution. Hereafter, we call such a laminated silicon steel sheet

† fukami@spring8.or.jp

ISBN: 978-3-95450-231-8 ISSN: 2673-5490 doi: 10.18429/JACoW-IPAC2023-WEODC2

core with insulating polyimide sheets the Double-layered Lamination Core (DLC).

We fabricated two kicker magnets with DLC and two conventional kicker magnets for comparison. In each type of kicker magnet, the laminated core was sandwiched between two glass epoxy plates of 32 mm thickness to maintain the shape of the core. The plates and the core were secured with four through bolts made of SUS316L covered with insulating polyimide sheets.

Table 1: Primary Parameter of the Test Kicker Magnets

Parameter	Value
Gap (mm)	22
Peak current (kA)	2.43
Peak voltage (kV)	8.7
Pole length (mm)	216
Integrated flux density (Tm)	0.06
Pulse width (μs)	3
Mismatch tolerance (%)	±0.1
Nominal inductance (μH)	3.8

TEST RESULT

Frequency Dependence of the Inductance

An LCR meter (NF Ltd., ZM2376) was used to measure the magnitude and phase of the impedance of the test kicker magnets over a frequency range of 100 Hz to 5 MHz. Consequently, the inductance of each magnet was calculated with the measured impedance. The obtained inductances of the two DLC and the two conventional magnets are shown as a function of the frequency in Fig.1. For each core type, the normalized inductance difference is defined as

$$\frac{\Delta L(f)}{L} \equiv \frac{L_{\#2}(f) - L_{\#1}(f)}{L_{\#1}(1kHz)}, \quad (1)$$

where $L_{\#1}(f)$ and $L_{\#2}(f)$ are the inductances at a frequency f of arbitrarily named magnets #1 and #2, respectively, and $L_{\#1}(1kHz)$ is the inductance of magnet #1 at 1 kHz. The normalized difference is also shown in the figure.

For both DLC and conventional, the difference can be resolved into two components: a constant offset component and a frequency-dependent component. The constant offset components were determined to be 0.07 % for the DLC magnets and 0.9 % for the conventional magnets. The constant offset components can be compensated by fine trimming of conductor lengths. In contrast, the frequency-dependent components were less than 0.1 % for the DLC magnets and 13.0 % for the conventional magnets in the 1 - 500 kHz frequency range. The frequency-dependent component can be caused by the difference in eddy currents induced on each magnet core. In the case of the conventional magnets, we hypothesized that the electrically contacting area on the edge of the laminated steel sheet in magnet #2 is larger than that in magnet #1.

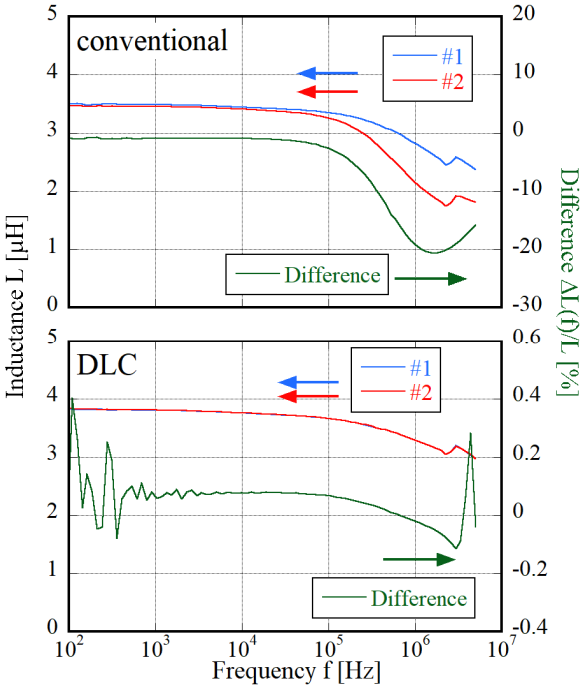

Figure 1: Measured frequency-dependent inductance of the two test magnets for the two core types and the difference between the two magnets of the same core type. The blue and red lines indicate the inductances of magnets #1s and #2s, respectively. The green line indicates the normalized inductance difference as defined in Eq.1. The upper panel shows the inductances for conventional magnets. The lower panel shows the inductances for DLC magnets.

Matching of the Pulsed Field Waveform

The matching of the pulsed field waveform between the two test magnets was investigated for each core type of DLC and conventional. The two test magnets were connected in parallel to one test power supply [14]. The integrated flux density was measured with a long search coil set along the beam axis on the median plane of the magnet. The search coil had a 460 mm long one-turn loop with an inner width of 0.5 mm and a line width of 0.1 mm patterned on a circuit board. The output voltage signal from the search coil was observed using an oscilloscope (LeCroy Ltd., WaveRunner 64Xi-A, 8-bit resolution), and the sampling interval was set to 1 ns. The integrated flux density was obtained by numerically integrating the sampled voltage signal.

The measured pulsed field waveforms of the two test magnets are shown in Fig.2. Sample-by-sample fluctuations in the measured field were observed. The ratio of the standard deviation of the fluctuation to the peak field was 0.02 %. For each core type, the normalized field difference is defined as

$$\frac{\Delta BL(t)}{BL} \equiv \frac{BL_{\#2}(t) - BL_{\#1}(t)}{BL_{\#1,peak}}, \quad (2)$$

where $BL_{\#1}(t)$ and $BL_{\#2}(t)$ are the integrated flux densities of magnets #1 and #2, respectively, and $BL_{\#1,peak}$ is the peak field of magnet #1. The normalized difference is also

ISBN: 978-3-95450-231-8 ISSN: 2673-5490 doi: 10.18429/JACoW-IPAC2023-WEODC2

shown in this figure. Considering the form of the difference, we estimated the delay and peak field difference between the two pulsed field waveforms. In the case of the conventional magnets, the timing of the peak of magnet #2 was delayed by 47 ns from that of magnet #1. The peak field of magnet #1 was 2.6 % higher than that of magnet #2. After numerical correction for the delay and the peak field difference, the recalculated normalized field difference remained at 2.3 % at the rising edge and 6.3 % at the undershoot region. In contrast, in the case of the DLC magnets, the delay was less than the data sampling interval. In addition, the peak field difference was less than the standard deviation of the sample-by-sample fluctuations. Furthermore, at any particular time during the pulse, the normalized difference was found to be within ±0.06 % for DLC. We confirmed that the mismatch of the pulsed field waveform between the two DLC kicker magnets was smaller than the required tolerance.

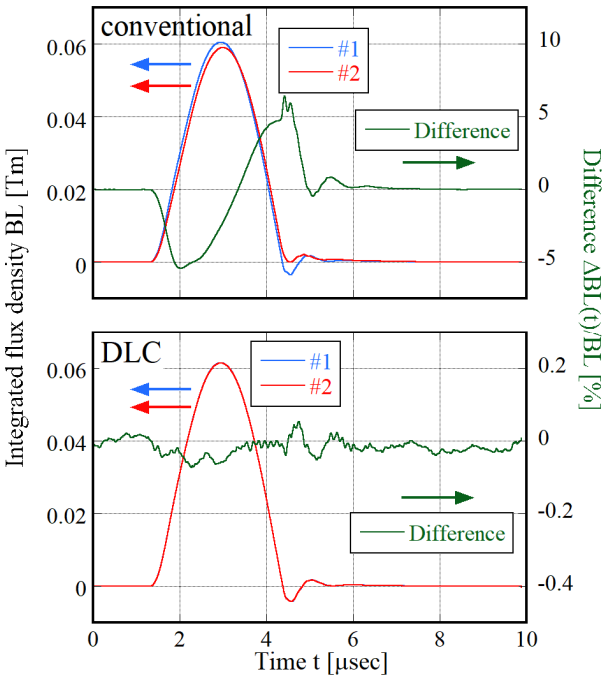

Figure 2: Measured pulsed field waveforms of the two test magnets for the two core types and the difference between the two test magnets of the same core type. The blue and red lines indicate integrated flux densities of #1s and magnet #2s, respectively. The green line indicates the normalized field difference as defined in Eq.2. The upper panel shows the fields for conventional magnets. The lower panel shows the fields for DLC magnets.

DISCUSSION

We investigated the inductance reduction observed in the test kicker magnets for the frequency region above 100 kHz. The reduction factor is defined as

$$R_f \equiv \frac{L(500kHz) - L(1kHz)}{L(1kHz)}, \qquad (3)$$

where *L(1kHz)* and *L(500kHz)* are the inductances at 1 kHz and 500 kHz, respectively. For the DLC magnet, the measured R_f was -9.6 % for both test magnets, whereas, for the conventional magnet, it was -12.4 % for magnet #1 and -25.7 % for magnet #2. To identify the cause of the inductance reduction in the high-frequency region, we quantitatively evaluated the inductance of the kicker magnet by calculating the magnetic field with the simulation code CST Studio, which provides a dynamic magnetic field analysis. The 3-dimensional flux density distribution was calculated assuming a periodical multi-layered core structure formed in the 0.1mm-thick steel sheet and the 0.025mm-thick polyimide sheet with infinite core length. The coil was excited by the sinusoidal current with frequencies of 1 kHz and 500 kHz. The inductance of the kicker magnet was evaluated from the calculated flux density integrated over an area surrounded by the coil.

We assumed perfect electric isolation between adjacent steel sheets and considered the conductivity of each steel sheet given in its specification sheet. Subsequently, the R_f was calculated to be -8.2 %. According to the specifications of ST-100, the thickness tolerances were +0.010 and -0.015 mm. Thus, the calculated R_f can be in the range of -9.0 % to -7.0 %. Note that an eddy current specific to the longitudinal core end is not included in the calculated value. The measured R_f for the DLC magnets was found to be marginally consistent with the simulation results. In contrast, we found that the extra inductance reduction observed in the conventional magnet can be attributed to imperfect electric isolation on the outer surfaces of the magnet core, resulting in an interlaminar short [13]. We concluded that the interlaminar insulating sheet of the DLC magnet surely insulates between steel sheets as we expected.

CONCLUSION

We have developed fast kicker magnets with the DLC. The most significant result of this work is that the magnetic field waveform of two kicker magnets, which can be extended to multiple kickers, is now an order of magnitude better matched than before. In addition, the iron lamination core has higher saturation flux density than the ferrite core. The DLC kicker magnets are expected to offer a promising solution to the demanding beam injection in modern and future light sources and colliders, where the ultimate stability of the stored beam is essential even at the time of top-up beam injection.

ACKNOWLEDGMENTS

This work was supported by the RIKEN SPring-8 Center (RSC) and the JST Next Generation Accelerator Technology Development Program. The authors thank TOKIN Co., Ltd. for carefully crafting the complicated DLC kicker magnets.

REFERENCES

[1] H. Tanaka *et al.*, "Suppression of injection bump leakage caused by sextupole magnets within a bump orbit", *Nucl. Instrum. Methods A*, Vol.539, 2005, pp. 547-557.

[2] T. Mouille, "Transient magnetodynamic finite element analysis of the ISIS M25/2 10Hz kicker magnet", in *Proc. 5th*

ISBN: 978-3-95450-231-8 ISSN: 2673-5490 doi: 10.18429/JACoW-IPAC2023-WEODC2

Int. Particle Accelerator Conf. (IPAC'14), Dresden, Germany, June 2014, pp.1313-1315. doi:10.18429/JACoW-IPAC2014-TUPR0112

[3] M. Mayer *et al*., "Steel tape-wound cut cores as magnet yokes for the beam-dump kickers of the large hadron collider", *IEEE Transactions on Magnetics*, Vol. 40, no. 4, 2004, pp. 3051-3053.

[4] S. White *et al*., "Damping of injection perturbations at the European Synchrotron Radiation Facility", *Phys. Rev. Accel. Beams*, Vol.22, no. 3, 2019, p. 032803.

[5] Y. Liu *et al*., "TPS SR kicker prototype installation status", in *Proc. 2nd Int. Particle Accelerator Conf. (IPAC'11)*, San Sebastian, Spain, Sep. 2011, paper THPC147, pp.3230-3232.

[6] N. Ogiwara *et al*., "Reduction of outgassing from the ferrite cores in the kicker magnet of J-PARC RCS", in *Proc. 3rd Int. Particle Accelerator Conf. (IPAC'12)*, New Orleans, LA, USA, May 2012, paper MOPPD053, pp. 487-489.

[7] C. Gough *et al*., "Septum and kicker systems for the SLS", in *Proc. Particle Accelerator Conf. (PAC'01)*, Chicago. U.S.A., June 2001, paper FPAH032, pp.3741-3743.

[8] http://www.nikkindenjikogyo.co.jp/english/Catalog-English.pdf

[9] https://product.tdk.com/system/files/dam/doc/product/ferrite/ferrite/ferrite-core/catalog/ferrite_mn-zn_material_characteristics_en.pdf

[10] H. Tanaka *et al*., "Stable top-up operation at SPring-8", *Journal of Synchrotron Radiation*, Vol. 13, no.5, 2006, pp. 378-391.

[11] T. Fan *et al*., "Magnetic field measurement on a refined kicker", in *Proc. Particle Accelerator Conf. (PAC'05)*, Knoxville, TN, USA, May 2005, paper MPPT020, pp. 1682-1684.

[12] P. Lebasque *et al*., "Four matched kicker systems for the SOLEIL storage ring injection, a full solid-state solution of pulsed power supplies working at high current", in *Proc. 10th European Particle Accelerator Conf. (EPAC'06)*, Edinburgh, UK, Jun. 2006, paper THPLS100, pp. 3508-3510.

[13] K. Fukami *et al*., "Iron lamination and interlaminar insulation for high-frequency pulsed magnets", *Review of Scientific Instruments*, 93, 023301, 2022.

[14] T. Inagaki *et al*., "Development of a solid-state pulse generator driving kicker magnets for a novel injection system of a low emittance storage ring", in *Proc. 9th Int. Particle Accelerator Conf. (IPAC'18)*, Vancouver, BC, Canada, Apr.-May 2018, pp.1804-1807. doi:10.18429/JACoW-IPAC2018-WEYGBF4